



# Periprosthetic bone quality affects the fixation of anatomic glenoids in total shoulder arthroplasty: in vitro study



Mohamad Chamseddine, MD<sup>1</sup>, Sebastian Breden<sup>1</sup>, Matthias F. Pietschmann, MD, Peter E. Müller, MD, Yan Chevalier, PhD\*

*Department of Orthopedic Surgery, Physical Medicine and Rehabilitation, Campus Grosshadern, University Hospital of Munich (Ludwig Maximilian University of Munich), Munich, Germany*

**Background:** Glenoid loosening, a common complication of shoulder arthroplasty, could relate to implant design and bone quality. However, the role of bone density has not been tested experimentally yet. In this study, tests on cadaveric specimens of varying bone density were performed to evaluate the effects of bone quality on loosening of typical anatomic glenoid implants.

**Methods:** Cadaveric scapulae scanned with a quantitative computed tomography scanner to determine bone mineral density (BMD) were implanted with either pegged or keeled cemented glenoid components and tested under constant glenohumeral load while a humeral head component was moved cyclically in the inferior and superior directions. Implant superior and inferior edge lifting, defined as displacement from the underlying bone, was measured with linear variable differential transducers until we reached 23,000 test cycles, and statistical testing was performed for differences in edge lifting due to implant design and related to periprosthetic BMD.

**Results:** Edge lifting was statistically significant at all time points, but on average, implant design had no effect. Lifting was highest in specimens in which BMD below the lifting edge was lower, with trends of increased displacement with decreased BMD.

**Conclusions:** Implant lifting was greater in glenoids of lower bone density for both implant designs. This finding suggests that fixation failure will most likely occur in bone of lower density and that the fixation design itself may play a secondary role.

**Level of evidence:** Basic Science Study; Biomechanics

© 2018 Journal of Shoulder and Elbow Surgery Board of Trustees. All rights reserved.

**Keywords:** Total shoulder arthroplasty; implant fixation; bone; clinical biomechanics; implant design; basic science study

This study was approved by our institutional ethical committee (Ethics Committee of Ludwig Maximilian University of Munich).

\*Reprint requests: Yan Chevalier, PhD, Department of Orthopedic Surgery, Physical Medicine and Rehabilitation, Campus Grosshadern, University Hospital of Munich (Ludwig Maximilian University of Munich), Marchioninistrasse 15, Munich D-81377, Germany.

E-mail address: [yan.chevalier@med.uni-muenchen.de](mailto:yan.chevalier@med.uni-muenchen.de) (Y. Chevalier).

<sup>1</sup>These authors contributed equally to this work.

The loosening of anatomic glenoid components remains the most common complication after total shoulder arthroplasty,<sup>3</sup> with rates of fixation failure that can reach up to 66% after 15 years.<sup>27</sup> Although the mechanisms of fixation failure are still unclear, it has been suggested that they relate in part to cementing techniques, component orientation and design, glenohumeral conformity,<sup>10,16,28</sup> or eccentric

loads occurring with shoulder instability.<sup>6</sup> Because the loosening ultimately involves a mechanical failure of the underlying interlocking of the cement and trabecular bone complex,<sup>14</sup> bone quality might also affect fixation and cement survival, particularly for low bone densities representative of and similar to the target patient population of glenoid replacement.<sup>5,11,18,23,26</sup>

The effects of cyclic eccentric loading on glenoid loosening have been suggested as one of the main factors affecting loosening.<sup>6</sup> This has been investigated experimentally based on a standard ASTM laboratory test developed after the work of Anglin et al<sup>1</sup> (2000), in which implanted glenoid components are subjected to cyclic superior-inferior motions of the humeral head under a constant glenohumeral load and edge displacements of the implant are measured. In most laboratory investigations of glenoid loosening, such tests are performed on synthetic bone surrogates.<sup>1,9,20,21,24</sup> Although this can be useful in quantifying the loosening differences between different implant fixation designs in a standardized manner, this may not adequately mimic the interfaces of the cement layer that occurs with natural bone, where surrounding marrow may prevent the optimal bond. Moreover, the use of synthetic bone may overlook the effects of bone density that occur in patients and the associated challenges in clinical practice. Recent studies involving cadaveric bones have been performed in combination with morphologic and micro-computed tomography (CT) analyses to identify failure mechanisms at the implant-cement-bone interfaces,<sup>8,13</sup> but they did not take into consideration how the bone density would affect the reported failures.

Numerical analyses have suggested that higher stresses in the cement layer and bone tissue may occur in glenoids of lower apparent bone density and heterogeneity.<sup>5</sup> In a recent numerical study by our group, the role of periprosthetic density and heterogeneity on cement and bone stresses was investigated. By use of micro-finite element models created from high-resolution peripheral quantitative computed tomography (QCT) scans of specimens implanted with pegged or keeled components, peak stresses were predicted at the cement-bone interface and trabecular bone tissue around the cemented zone.<sup>5</sup> A similar study using classical finite element analysis also demonstrated how lower periprosthetic bone density can lead to higher internal stresses and increased risk of fixation failure.<sup>26</sup> However, such an effect was not yet accounted for experimentally, which motivated the present study. Furthermore, no comparison between different fixation designs has yet been made using the direct measurement of edge displacements in relation to periprosthetic bone density. In fact, in most studies in which fixation designs were compared, the studies were again performed on synthetic materials rather than cadaveric specimens.<sup>1,9,20,24</sup> It is therefore still unknown whether edge displacements will significantly differ when tested in cadaveric bone specimens that better mimic clinical implantation conditions and whether bone density in the implantation regions may explain potential differences in fixation movement.

In this study, we hypothesized that risks of implant lifting and therefore loosening are increased with decreasing bone density below the component for 2 common cemented implant designs. We also hypothesized that bone mineral density (BMD) could reveal differences in the measured lifting owing to fixation design. To test these hypotheses, a series of cadaveric scapulae were tested in a new dynamic setup after the implantation of keeled and pegged glenoid components, and edge lifting of the implants was related to bone density in periprosthetic bone regions measured with QCT scanning of the specimens.

## Methods

### Specimen preparation

In this cadaveric biomechanical study, 6 pairs of fresh-frozen cadaveric shoulder specimens (mean age,  $69 \pm 13$  years; 4 male and 2 female cadavers) without macroscopic signs of osteoarthritis, trauma, or the presence of osteophytes or bone deformity were obtained from our institution. The scapulae were extracted and cleaned of soft tissues with the acromion resected and cut 10 cm from the center of the glenohumeral joint surface. Glenoid dimensions were measured by caliper in the superior-inferior ( $39.2 \pm 2.4$  mm) and anterior-posterior ( $27.8 \pm 2.8$  mm) directions.

### QCT scanning and image analysis

The specimens were then scanned using a clinical QCT scanner (47 mA, 100 kV) (Sensation 64 Somatom; Siemens, Munich, Germany), with an in-plane resolution of 0.346 mm and a slice thickness of 1 mm. The images were resampled to an isometric resolution of 0.346 mm and processed with custom Python and Fortran codes<sup>4</sup> to quantify BMD (in milligrams of hydroxyapatite (HA) per cubic centimeter) in the glenoid, after conversion from Hounsfield units to BMD using the calibration phantom included in the CT images. Specifically, semiautomatic image segmentation allowed the outer glenoid bone contours to be defined. Then, an algorithm was used to fill the bone region inside this outer contour and to mask out the surrounding voxels. The images were cropped up to 30 mm from the middle of the glenoid articular surface, which allowed for standardization of the amount of bone below the fixation features of the components. Three main regions were defined: the full glenoid region, an inner bone region obtained by eroding the segmented images by 0.7 mm, and a 0.7-mm peripheral bone region including the cortical shell obtained by subtraction of the inner bone region from the full glenoid region. Finally, each bone region was divided into superior and inferior zones using the middle of each glenoid joint surface as a transversal cutting plane. Mean local BMD values were then calculated for each zone (Fig. 1).

### Anatomic glenoid implantation procedure

We divided the specimen pairs into 2 equal groups, and an experienced surgeon (M.F.P.) randomly implanted the left or right side with either a pegged ( $n = 6$ ) or keeled ( $n = 6$ )

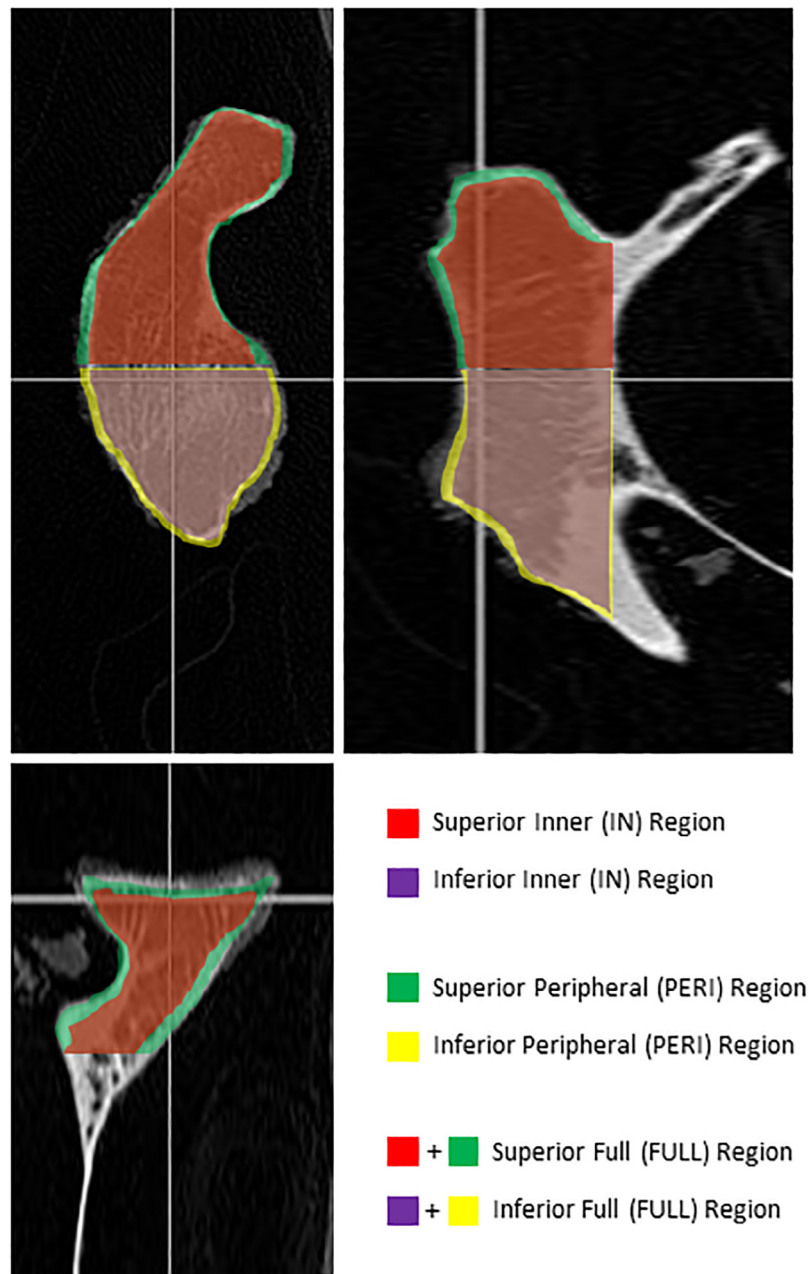


**Figure 1** Computed tomography images of cadaveric scapula specimens before implantation in 3 anatomic views. After segmentation of the bone contour and exclusion of the outer 1 mm, inferior and superior inner (*IN*), peripheral (*PERI*), and full (*FULL*) bone regions were defined by splitting the glenoid midway at the articular surface and cropping 30 mm from the articular surface. This allowed calculation of regional inferior and superior bone mineral density.

ultrahigh-molecular-weight polyethylene, anatomic glenoid replacement (alpha curvature medium models; Exactech, Gainesville, FL, USA) using standard implantation and cementing techniques. Implantations were performed without correcting for version or tilt. Glenoid articular surfaces were reamed by 4 mm in a direction normal to the glenoid surface, and peg or keel holes were drilled and subsequently filled with a layer of cement (PALACOS MV+G; Heraeus Medical, Wehrheim, Germany). Cement was also applied on the component's back before implantation.

### Cyclic testing setup

The specimens were embedded at the scapular blade in an aluminum pot 5 cm away from the joint with polymethyl methacrylate (Technovit; Kulzer, Hanau, Germany), with the center of the articulation surface of the implant component carefully aligned vertically. This pot was then mounted on a custom biaxial testing setup (Fig. 2), based on the rocking-horse ASTM F 2808-02 testing standard,<sup>2</sup> which was developed to simulate constant

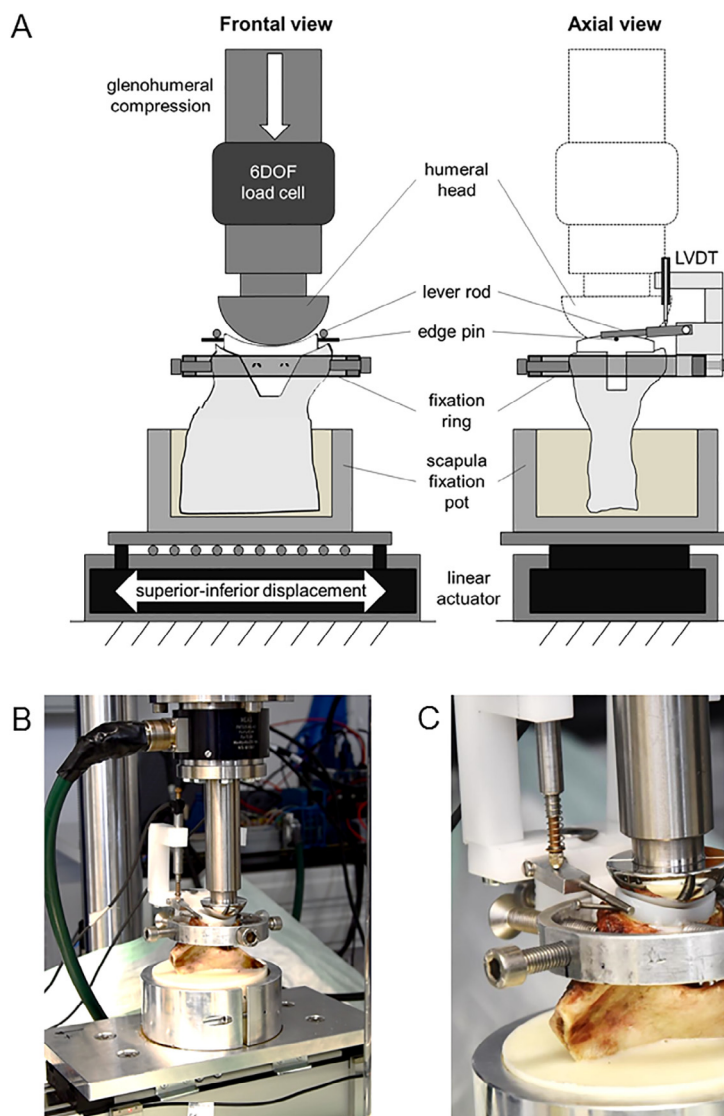


**Figure 2** Schematic frontal and axial views (A) and photographs (B, C) of cyclic loading apparatus to test anatomic glenoid components implanted in cadaveric bone under constant glenohumeral load with dynamic cyclic superior-inferior displacement of humeral head. A ring was rigidly fixed to the bone near the implant edge, and linear variable differential transducers (LVDT), in contact with lever arms lying on pins fixed on the superior and inferior sides of the implant, allowed measurement of edge lifting. *DOF*, degrees of freedom.

glenohumeral load in the vertical direction while the specimen was moved cyclically in the inferior and superior directions with a horizontal linear actuator (RK DuoLine S 80; Phoenix Mecano, Stein am Rhein, Switzerland). The glenoid component was put in contact with a prosthetic humeral head mounted on the vertical actuator of a dynamic hydraulic system (ElectroPuls E10000; Instron, Norwood, MA, USA), through a 6-*df* load cell (MEAS Q110U1; Disynet, Brügglen, Germany), capable of measuring linear loads and rotational moments. A humeral head (Exactech) was selected with a diameter of 41 mm, providing a glenohumeral mismatch of 5.5 mm.

Threaded pins of 1 cm in length were screwed into the superior and inferior sides of the glenoid implants. An aluminum ring was fixed rigidly to the scapula 1 cm below the glenohumeral joint. Medially aligned linear variable differential transducers (LVDTs) (WETA 1/2m; HBM, Darmstadt, Germany) were mounted on the frame so that their tips were in contact with lever arms resting on the infe-

rior and superior threaded pins near the implant edges. Implant edge lifting, defined as displacement of the superior and inferior glenoid edges relative to the bone, was then recorded with LabVIEW software (2014 version; National Instruments, Austin, TX, USA).

## Testing

A constant glenohumeral load of 350 N was applied at all times based on another subluxation study.<sup>25</sup> This load is lower than the ASTM standard<sup>2</sup> but was chosen to avoid specimen failure that occurred in a previous preliminary sample while preparing for the present study. The tests were conducted in 2 phases. First, the specimens were moved inferiorly or superiorly with the humeral head in loaded contact until the maximum shear loads in those directions were detected, as measured with the 6-*df* load cell. The superior or inferior head displacements corresponding to these maximum shear loads were

simultaneously measured with an LVDT aligned in the superior-inferior direction and were defined as the subluxation limits.

Subsequently, a rocking cyclic test was performed with the same constant glenohumeral load while the scapula was cyclically displaced at 0.25 Hz in the superior-inferior direction, within 90% of the previously measured specimen-specific subluxation limits, for up to 23,000 cycles, corresponding to approximately 1 day of testing. The combination of constant glenohumeral load and dynamic superior-inferior displacement resulted in an average superior-inferior subluxation range of  $24 \pm 2$  mm and a corresponding shear load of  $303 \pm 19$  N in the superior-inferior direction. The relative mediolateral displacements at the superior and inferior implant edges, defined as superior edge lifting and inferior edge lifting, respectively, were recorded with 2 LVDTs at cycles 1000, 4000, and 23,000.

## Statistical tests

Edge lifting was tested at each measurement point of 1000, 4000, and 23,000 cycles for statistical differences (Wilcoxon [Mann-Whitney] test) in relation to implant design and the reference initial measurement of lifting. Edge lifting was further related with linear correlations to the QCT-based measurements of BMD in each of the periprosthetic bone regions. Statistical significance was assumed for  $P < .05$ .

## Morphologic studies

After all tests, the glenoids were separated from each scapula close to the implants using a diamond band saw (Diamant-Trennschleifsystem cut-grinder; Patho-Service, Oststeinbek, Germany). The glenoids were then cut in the inferior-superior direction through the center of each implant to generate one anterior half and one posterior half. Subsequently, each half was scanned using a contact x-ray scanner (Faxitron; Hewlett-Packard, Wilmington,

DE, USA). These contact radiographic images were inspected for radioluminescence that can be related to bone failure. In addition, the 2 cut surfaces of each specimen were photographed for further evaluation. The images were inspected for gaps at the interfaces between bone, cement, and implant, as well as for bone tissue and cement mantle fractures.

## Results

Early bone failure occurred near the embedment in 1 specimen, and the pair was discarded from the study. No apparent cortical bone failure was observed between the implant and fixation ring of the LVDT measurement system in the remaining specimens.

The age, sex, and glenoid dimensions of the remaining specimens, along with their subregional bone density, are presented in Table I. Mean BMD in the superior and inferior inner bone regions was  $269 \pm 30$  mg HA/cm<sup>3</sup> and  $273 \pm 33$  mg HA/cm<sup>3</sup>, respectively, for the keeled design and  $263 \pm 36$  mg HA/cm<sup>3</sup> and  $232 \pm 34$  mg HA/cm<sup>3</sup>, respectively, for the pegged design. No statistical differences were revealed either between the BMD values in the keeled and pegged groups or between the inferior and inner BMD values of each glenoid design.

Lifting displacements generally increased with the number of cycles in both superior and inferior glenoid edges and for both implant designs (Fig. 3). On average, for the entire series of successfully tested specimens, inferior edge lifting and superior edge lifting were significant and different from zero for all measurement points ( $P = .013$  for keeled design and  $P = .005$  for pegged design). After 4000 cycles, measurements of mean edge lifting for the keeled design were slightly higher in the inferior edge than the superior edge; in contrast,

**Table I** Details of tested specimens

	Donor sex	Donor age of death, yr	Implant design	Glenoid dimensions, cm		Implant size	Trabecular BMD, mg HA/cm <sup>3</sup>	
				SI	AP		Inferior	Superior
Specimen pair								
1*	Female	84	Keeled	3.7	2.7	Medium	266	277
			Pegged	3.7	2.5	Medium	179	274
2	Male	79	Keeled	4.2	3.3	Large	253	251
			Pegged	4.0	3.0	Large	226	202
3	Male	69	Keeled	4.0	3.0	Large	243	234
			Pegged	4.0	3.0	Large	245	267
4	Male	51	Keeled	4.0	3.0	Large	304	293
			Pegged	4.3	2.8	Large	257	246
5	Male	55	Keeled	4.0	2.5	Medium	324	312
			Pegged	4.0	2.6	Medium	272	308
6	Female	78	Keeled	3.6	2.4	Medium	249	249
			Pegged	3.5	2.5	Medium	211	281
Mean for keeled design*							$273 \pm 33$	$269 \pm 30$
Mean for pegged design*							$232 \pm 34$	$263 \pm 36$

BMD, bone mineral density; HA, hydroxyapatite; SI, superior-inferior dimension; AP, anterior-posterior dimension.

\* Pair 1 was excluded from the study after early bone failure of 1 of the 2 specimens at the embedment. Means and standard deviations for the pegged and keeled design groups were calculated after exclusion of pair 1.

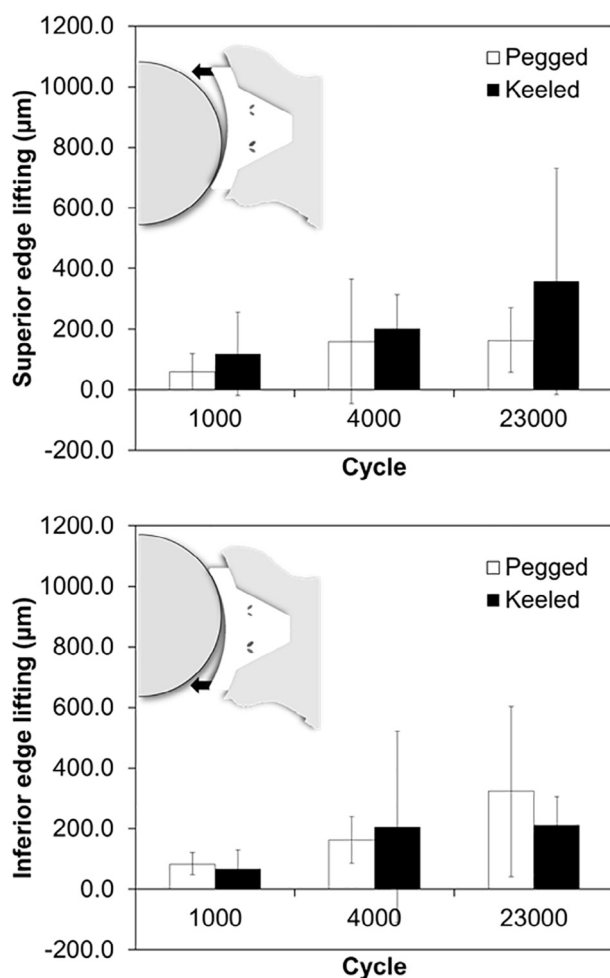


**Figure 3** Mean superior and inferior edge lifting (←) for keeled and pegged fixation designs at 3 measurement times. The vertical lines are standard deviations.

these were 50% lower in the inferior edge than the superior edge for the pegged design. At the end of the tests, lifting increased on average by 82% in the superior edge of the keeled components and by 185% in the inferior edge of the pegged components. Although slightly higher lifting values were observed for the keeled design, no statistically significant differences in edge displacements due to implant design were observed at all time points ( $P = .056$ ).

Lifting was seen to be generally affected by BMD in both periprosthetic zones, reaching as much as 1000 µm for specimens of lower bone density, whereas distractions of less than 200 µm were measured in the denser bone specimens (Figs. 4 and 5). Differences could also be observed depending on implant fixation design; for the keeled design, generally higher lifting occurred at the superior edge than the inferior edge, whereas for the pegged design, lifting was greater at the inferior edge. Trends of increased displacement were observed with decreased BMD (Table II). In particular, for the pegged design, inferior edge lifting correlated with inferior inner BMD ( $R^2 = 0.771$ ,  $P = .049$ ) and superior edge lifting correlated with inferior peripheral BMD ( $R^2 = 0.898$ ,  $P = .014$ ). For the keeled

design, inferior edge lifting correlated with both full inferior and superior BMD ( $R^2 = 0.80$ ,  $P = .040$ ).

At the tissue level, no macroscopic fractures or cracks of the bone or cement mantle were found in any of our specimens on visual inspection. Gaps at the interfaces were also not noticeable from the photographs. Further contact radiographic analysis of the specimens did not reveal any trabecular microfracture in the form of radiolucency (Fig. 6).

## Discussion

This study aimed to test our hypotheses that fixation design and bone quality can affect the fixation stability of anatomic cemented glenoid components used in total shoulder arthroplasty and implanted in cadaveric specimens. Our first hypothesis, that bone quality would affect the fixation stability of the components, is validated by our findings showing that edge lifting for both designs increased with decreasing bone density. In specimens of lower trabecular bone density, peak lifting values of nearly 800 µm could be measured, whereas after a similar testing duration, specimens with higher inner bone density showed edge lifting reduced by a factor of 4. This was generally more apparent after 23,000 test cycles, but significant trends of edge lifting with decreasing bone density could also be evidenced after only 4000 cycles. It is therefore reasonable to assume that testing for longer durations would have accentuated these trends, at least in this study on cadaveric specimens.

Our second hypothesis was that bone density not only would affect fixation stability but also could reveal differences due to implant fixation designs. Although, on average, for all specimens, displacements did not show statistical differences between implant fixation designs at any measurement time, some differences were indeed revealed by accounting for bone density in the inner bone regions, validating this hypothesis. The keeled design showed higher lifting at its superior edge than at its inferior edge for lower BMD in both zones. On the other hand, for the pegged design, edge lifting was higher on the inferior side in specimens of lower bone density and, particularly, in the inferior trabecular region. For components cemented in higher-density periprosthetic bone, the edge lifting amounts were considerably reduced and these differences in design appeared to be less important. Because no statistical differences were observed between the different bone regions in our specimens, we suspect that such differences in edge lifting may rely on the fixation design. The higher superior distractions measured for the keeled design in weaker bone, in combination with higher trabecular bone tissue stresses in the superior region predicted by our previous numerical micro-finite element analyses,<sup>5</sup> suggest that although overall bone quality may affect pegged designs, bone quality in the superior region may play a larger role in the fixation of keeled designs.

To our knowledge, this study is the first to investigate the role of bone density on edge lifting of such prosthetic

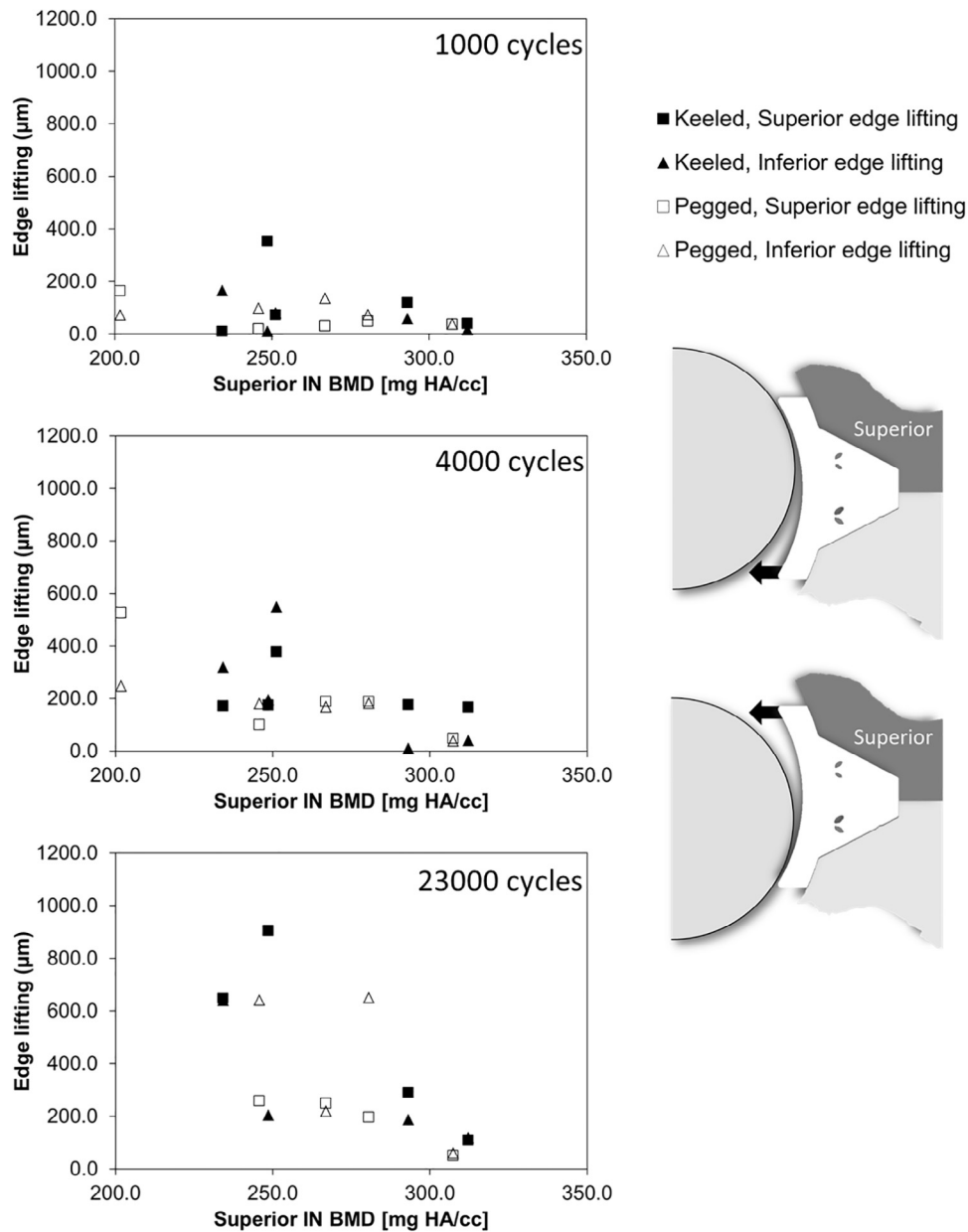


**Figure 4** Edge lifting ( $\leftarrow$ ) for both keeled and pegged fixation designs in terms of bone mineral density (*BMD*) in superior periprosthetic inner (*IN*) bone region at 1000, 4000, and 23,000 cycles. *HA*, hydroxyapatite.

components tested in a dynamic cyclic scheme and implanted in cadaveric specimens. This is particularly important considering the limited bone stock available in the glenoid cavity, as well as local variations that have been reported between the inferior and superior regions.<sup>12</sup> Because there is minimal bone stock available at the glenoid, fixation of cemented implants should account for reported regional variations in bone density. In our study, no differences between inferior and superior regional inner *BMD* values were observed on average, but past experiments suggested higher density and mechanical strength in central areas of the superior and posterior regions.<sup>7,12</sup> In lower-density bone, increased compliance and microdamage can be expected with cyclic loading, leading

to weakened fixation. During compression, the pegged design provides greater anchorage in the inferior part than the keeled design with pegs that might distribute loads closer to the stronger, denser cortical shell.<sup>5</sup> In particular, in low-density trabecular bone, these pegs may help reduce peak loads in the trabecular bone tissue and cement layer, as well as limit distraction on the opposite superior edge, compared with the keeled design. However, it is yet unknown how local bone anisotropy varies with overall density at the glenoid and how this contributes to the fixation stability of both designs.

In addition, the specimens were sectioned and inspected to identify failure regions. From these tested samples, it was not possible, using visual inspection of

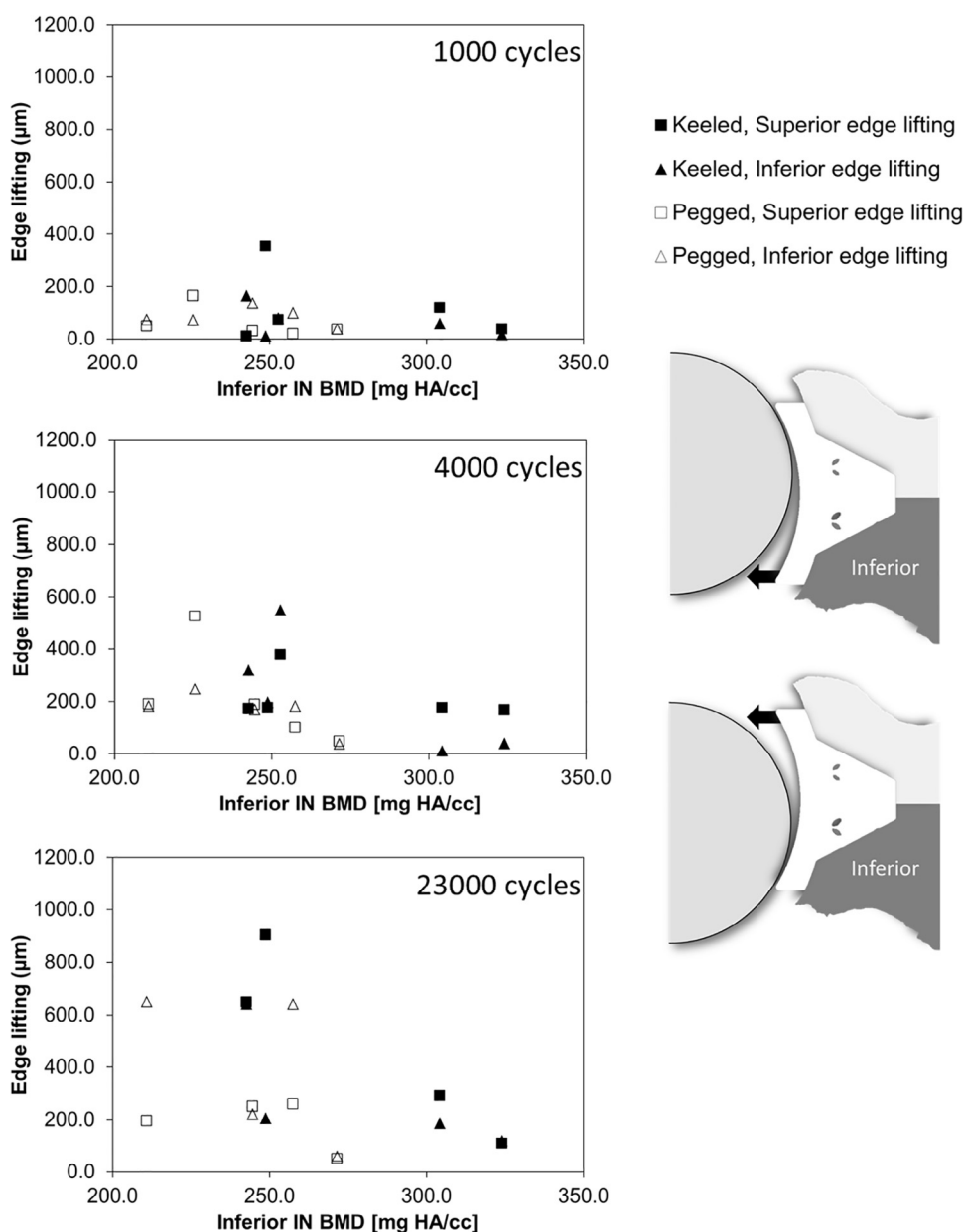


**Figure 5** Edge distractions ( $\leftarrow$ ) for both keeled and pegged fixation designs in terms of bone mineral density (*BMD*) in inferior periprosthetic inner (*IN*) bone region at 1000, 4000, and 23,000 cycles. *HA*, hydroxyapatite.

photographs and contact radiographs, to clearly identify the exact location of implant fixation failure initiation. This kind of comparison has in recent studies proved to be difficult and may rely on high-resolution micro-CT scanning for a better assessment.

As with most cadaver-based experimental studies, some factors may limit the extension of these findings to the clinical setting. First, only 6 specimen pairs were used in this study, and only 5 pairs were tested successfully. Although this number was sufficient to show significant displacements at every measurement point and the measured range of bone density was large enough to reveal trends of increased displacement with decreasing bone density, more specimens would be

required to improve the significance of the reported relationships between distractions and local periprosthetic bone quality for each tested design. Second, because of the difficulty of obtaining pathologic cadaveric specimens, those used in this study did not present potential morphologic, subchondral, and microstructural trabecular bone changes that can be expected in arthritic glenoids. How such factors can influence edge displacements is still unknown. Furthermore, this study used load magnitudes that were smaller than the typical test standards for synthetic materials.<sup>1,9,19,21</sup> This was done for practical reasons because our specimens were not fully embedded to avoid overconstraining bone structures around the implant and to allow sufficient space near the joint surface to fix the

**Table II** Correlation coefficients ( $R^2$ ) and  $P$  values for relationships between edge lifting and periprosthetic BMD

BMD region and fixation design	$R^2$ value ( $P$ value)			
	4000 cycles		23,000 cycles	
	Inferior edge lifting	Superior edge lifting	Inferior edge lifting	Superior edge lifting
Inner				
Keel				
Inferior	0.575 (.137)	0.117 (.572)	0.504 (.290)	0.875 (.065)
Superior	0.545 (.154)	0.088 (.629)	0.600 (.225)	0.804 (.103)
Pegged				
Inferior	0.521 (.169)	0.374 (.273)	0.387 (.378)	0.169 (.589)
Superior	0.771 (.049*)	0.719 (.070)	0.429 (.345)	0.876 (.064)
Keel and pegged				
Inferior	0.270 (.345)	0.132 (.064)	0.418 (.083)	0.100 (.446)
Superior	0.395 (.049*)	0.439 (.037*)	0.434 (.075)	0.544 (.037*)
Peripheral				
Keel				
Inferior	0.410 (.245)	0.669 (.091)	0.065 (.744)	0.334 (.422)
Superior	0.233 (.410)	0.477 (.197)	0.153 (.609)	0.259 (.491)
Pegged				
Inferior	0.522 (.168)	0.898 (.014*)	0.777 (.119)	0.097 (.689)
Superior	0.538 (.159)	0.462 (.207)	0.499 (.294)	0.344 (.413)
Keel and pegged				
Inferior	0.437 (.037*)	0.358 (.068)	0.003 (.893)	0.237 (.221)
Superior	0.290 (.108)	0.306 (.097)	0.000 (.970)	0.290 (.168)
Full				
Keel				
Inferior	0.939 (.007*)	0.689 (.082)	0.319 (.435)	0.841 (.083)
Superior	0.808 (.038*)	0.392 (.259)	0.294 (.458)	0.473 (.312)
Pegged				
Inferior	0.009 (.876)	0.034 (.768)	0.272 (.478)	0.074 (.728)
Superior	0.110 (.585)	0.086 (.632)	0.020 (.858)	0.199 (.553)
Keel and pegged				
Inferior	0.210 (.183)	0.096 (.384)	0.002 (.921)	0.004 (.882)
Superior	0.108 (.355)	0.106 (.357)	0.004 (.888)	0.012 (.794)

BMD, bone mineral density.

\* Statistically significant ( $P < .05$ ).

measurement system. This, however, resulted in higher shear and bending loads at the scapular bone than in tests in which synthetic or cadaveric bones were embedded closer to the joint. To avoid potential specimen failure at the embedment that occurred in 1 pilot specimen, lower loads levels were used, based on a previous subluxation study on cadaveric specimens.<sup>25</sup> In addition, this cadaveric study does not account for biological factors and wear-related bone osteolysis, which are expected to regulate bone response in vivo and which might affect the stiffness of the cement-bone interface.<sup>17,22</sup> Moreover, the study was performed under a reduced duration and frequency compared with tests on synthetic materials, mainly to limit testing to 1 day and avoid degradation of inert biological tissues that might differ from the in vivo conditions, in which bone remodeling is expected to take place. Nevertheless, the observed edge displacements after 23,000 cycles reached almost 1 mm for the weaker bone specimens, whereas limited amounts of displacement could be observed for

stronger specimens. Furthermore, general trends of increased edge distractions with decreasing periprosthetic BMD could be observed even at 4000 cycles. We therefore believe that longer durations will accentuate the already observed trends. In addition, testing was limited to the superior-inferior direction, but anterior-posterior rocking mimicking eccentric loads that can also occur in vivo<sup>15</sup> might reveal additional differences in fixation stability based on design when accounting for local periprosthetic bone quality. Another limitation comes from the fact that specimens were tested in a standardized orientation, without accounting for biomechanical changes in loading due to variations in version and tilt angles. Future work will be needed to assess these effects on glenoid fixation. Finally, our study did not investigate the failure mode as has been done in published methodologies with histologic evaluation and micro-CT imaging.<sup>8,13</sup> Because this study was based on the rocking test protocol to assess fixation loosening, loading involved compression and lifting

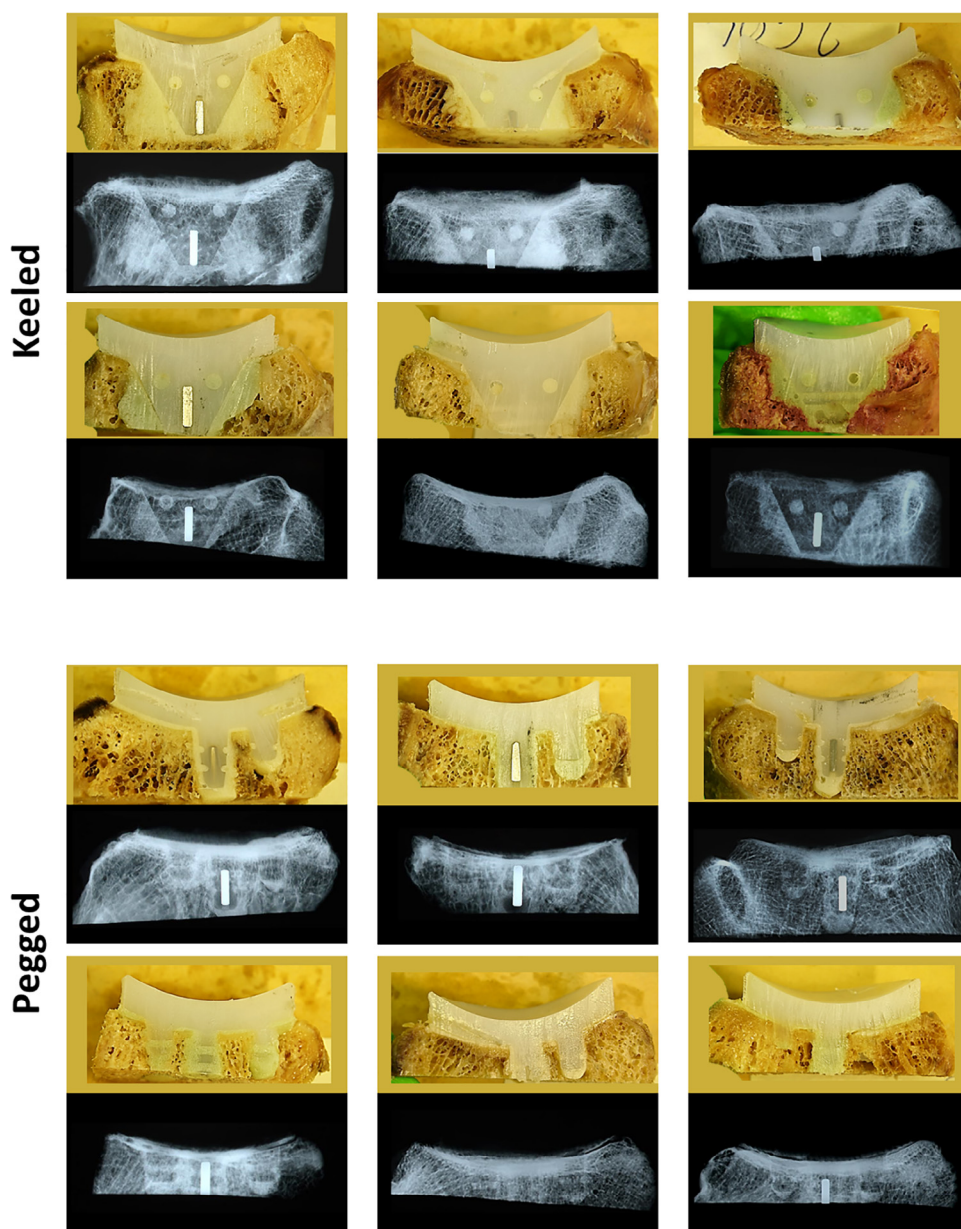


**Figure 6** Photographic and contact radiographic images for 12 specimens after rocking-horse testing.

on each edge, resulting in an end state that may not reflect the measured peak implant lifting.

### Conclusion

Despite these limitations, our results, obtained from cadaveric bones rather than synthetic materials to more adequately simulate clinical implantation conditions, showed that available bone quality at the implantation site may be a crucial determinant of fixation failure and should be accounted for in improving current fixation. For keeled implants, the results showed higher lifting of the superior edge than the inferior edge in lower-density bone, which

is opposite to the observations in pegged implants. Our study further showed that displacements are reduced for components implanted in higher-density glenoids. Definitive answers to the question of whether periprosthetic bone density has a role in loosening of glenoid components in anatomic total shoulder arthroplasty will require a retrospective clinical study.

### Disclaimer

Prosthetic components were provided by Exactech free of charge.

The authors, their immediate families, and any research foundations with which they are affiliated have not received any financial payments or other benefits from any commercial entity related to the subject of this article.

## References

1. Anglin C, Wyss UP, Pichora DR. Mechanical testing of shoulder prostheses and recommendations for glenoid design. *J Shoulder Elbow Surg* 2000;9:323-31.
2. ASTM F 2028-02. Standard test methods for the dynamic evaluation of glenoid loosening or dissociation. In: Book of ASTM standards. Conshohocken, PA: ASTM International; 2004. p. 1083-8.
3. Bohsali KI, Wirth MA, Rockwood CA Jr. Complications of total shoulder arthroplasty. *J Bone Joint Surg Am* 2006;88:2279-92. <http://dx.doi.org/10.2106/JBJS.F.00125>
4. Chevalier Y. Numerical methodology to evaluate the effects of bone density and cement augmentation on fixation stiffness of bone-anchoring devices. *J Biomech Eng* 2015;137. <http://dx.doi.org/10.1115/1.4030943>
5. Chevalier Y, Santos I, Müller PE, Pietschmann MF. Bone density and anisotropy affect periprosthetic cement and bone stresses after anatomical glenoid replacement: a micro finite element analysis. *J Biomech* 2016;49:1724-33. <http://dx.doi.org/10.1016/j.jbiomech.2016.04.003>
6. Franklin JL, Barrett WP, Jackins SE, Matsen FA III. Glenoid loosening in total shoulder arthroplasty. Association with rotator cuff deficiency. *J Arthroplasty* 1988;3:39-46.
7. Frich LH, Jensen NC, Odgaard A, Pedersen CM, Sjøbjerg JO, Dalstra M. Bone strength and material properties of the glenoid. *J Shoulder Elbow Surg* 1997;6:97-104.
8. Gregory T, Hansen U, Taillieu F, Baring T, Brassart N, Mutchler C, et al. Glenoid loosening after total shoulder arthroplasty: an in vitro CT-scan study. *J Orthop Res* 2009;27:1589-95. <http://dx.doi.org/10.1002/jor.20912>
9. Gunther SB, Lynch TL, O'Farrell D, Calyore C, Rodenhouse A. Finite element analysis and physiologic testing of a novel, inset glenoid fixation technique. *J Shoulder Elbow Surg* 2012;21:795-803. <http://dx.doi.org/10.1016/j.jse.2011.08.073>
10. Karelse A, Van Tongel A, Van Isacker T, Berghs B, De Wilde L. Parameters influencing glenoid loosening. *Expert Rev Med Devices* 2016;13:773-84. <http://dx.doi.org/10.1080/17434440.2016.1205483>
11. Lacroix D, Murphy LA, Prendergast PJ. Three-dimensional finite element analysis of glenoid replacement prostheses: a comparison of keeled and pegged anchorage systems. *J Biomech Eng* 2000;122:430-6.
12. Lehtinen JT, Tingart MJ, Apreleva M, Warner JJ. Total, trabecular, and cortical bone mineral density in different regions of the glenoid. *J Shoulder Elbow Surg* 2004;13:344-834. <http://dx.doi.org/10.1016/j.jse.2004.01.012>
13. Lewis GS, Brenza JB, Paul EM, Armstrong AD. Construct damage and loosening around glenoid implants: a longitudinal micro-CT study of five cadaver specimens. *J Orthop Res* 2016;34:1053-60. <http://dx.doi.org/10.1002/jor.23119>
14. Mann KA, Miller MA, Cleary RJ, Janssen D, Verdonschot N. Experimental micromechanics of the cement-bone interface. *J Orthop Res* 2008;26:872-9. <http://dx.doi.org/10.1002/jor.20575>
15. Massimini DF, Li G, Warner JP. Glenohumeral contact kinematics in patients after total shoulder arthroplasty. *J Bone Joint Surg Am* 2010;92:916-26. <http://dx.doi.org/10.2106/JBJS.H.01610>
16. Matsen FA III, Clinton J, Lynch J, Bertelsen A, Richardson ML. Glenoid component failure in total shoulder arthroplasty. *J Bone Joint Surg Am* 2008;90:885-96. <http://dx.doi.org/10.2106/JBJS.G.01263>
17. Miller MA, Eberhardt AW, Cleary RJ, Verdonschot N, Mann KA. Micromechanics of postmortem-retrieved cement-bone interfaces. *J Orthop Res* 2010;28:170-7. <http://dx.doi.org/10.1002/jor.20893>
18. Patel RJ, Gulotta L, Wright TM, Gao Y. Effects of osteoarthritis on load transfer after cemented total shoulder arthroplasty. *J Shoulder Elbow Surg* 2015;24:407-15. <http://dx.doi.org/10.1016/j.jse.2014.08.011>
19. Roche C, Angibaud L, Flurin PH, Wright T, Zuckerman J. Glenoid loosening in response to dynamic multi axis eccentric loading: a comparison between keeled and pegged designs with an equivalent radial mismatch. *Bull Hosp Jt Dis* 2006;63:88-92.
20. Sabesan VJ, Ackerman J, Sharma V, Baker KC, Kurdziel MD, Wiater JM. Glenohumeral mismatch affects micromotion of cemented glenoid components in total shoulder arthroplasty. *J Shoulder Elbow Surg* 2015;24:814-22. <http://dx.doi.org/10.1016/j.jse.2014.10.004>
21. Sarah J, Sanjay G, Sanjay S, Carolyn A, Emery R, Andrew A, et al. Failure mechanism of the all-polyethylene glenoid implant. *J Biomech* 2010;43:714-9. <http://dx.doi.org/10.1016/j.jbiomech.2009.10.019>
22. Strauss EJ, Roche C, Flurin PH, Wright T, Zuckerman JD. The glenoid in shoulder arthroplasty. *J Shoulder Elbow Surg* 2009;18:819-33. <http://dx.doi.org/10.1016/j.jse.2009.05.008>
23. Stroud NJ, DiPaola MJ, Martin BL, Steiler CA, Flurin PH, Wright TW, et al. Initial glenoid fixation using two different reverse shoulder designs with an equivalent center of rotation in a low-density and high-density bone substitute. *J Shoulder Elbow Surg* 2013;22:1573-9. <http://dx.doi.org/10.1016/j.jse.2013.01.037>
24. Suárez DR, Nerkens W, Valstar ER, Rozing PM, van Keulen F. Interface micromotions increase with less-conforming cementless glenoid components. *J Shoulder Elbow Surg* 2012;21:474-82. <http://dx.doi.org/10.1016/j.jse.2011.03.008>
25. Tammachote N, Sperling JW, Berglund LJ, Steinmann SP, Cofield RH, An KN. The effect of glenoid component size on the stability of total shoulder arthroplasty. *J Shoulder Elbow Surg* 2007;16:S102-6. <http://dx.doi.org/10.1016/j.jse.2006.03.012>
26. Terrier A, Obrist R, Becce F, Farron A. Cement stress predictions after anatomic total shoulder arthroplasty are correlated with preoperative glenoid bone quality. *J Shoulder Elbow Surg* 2017;26:1644-52. <http://dx.doi.org/10.1016/j.jse.2017.02.023>
27. Young A, Walch G, Boileau P, Favard L, Gohlke F, Loew M, et al. A multicentre study of the long-term results of using a flat-back polyethylene glenoid component in shoulder replacement for primary osteoarthritis. *J Bone Joint Surg Br* 2011;93:210-6. <http://dx.doi.org/10.1302/0301620X.93B2.25086>
28. Zhang J, Yongpravat C, Kim HM, Levine WN, Bigliani LU, Gardner TR, et al. Glenoid articular conformity affects stress distributions in total shoulder arthroplasty. *J Shoulder Elbow Surg* 2013;22:350-6. <http://dx.doi.org/10.1016/j.jse.2012.08.025>